

## Supplementary Information

### **Laser induced trace doping of Pd on Ru nanoparticles for efficient hydrogen evolution electrocatalyst**

Ziang Guo,<sup>‡a</sup> Liye Zhu,<sup>‡a</sup> Xuan Liu,<sup>a,b,c,d</sup> Ran Zhang,<sup>a</sup> Tiying Zhu,<sup>a</sup> Nan Jiang,<sup>a</sup>  
Yan Zhao<sup>\*a,b,c,d</sup> and Yijian Jiang<sup>a,b,c,d</sup>

<sup>a</sup>Institute of Laser Engineering, Faculty of Materials and Manufacturing, Beijing University of Technology, Beijing 100124, People's Republic of China.

<sup>b</sup>Key Laboratory of Trans-scale Laser Manufacturing Technology (Beijing University of Technology), Ministry of Education, Beijing 100124, People's Republic of China.

<sup>c</sup>Beijing Engineering Research Center of Laser Technology, Beijing University of Technology, Beijing 100124, People's Republic of China.

<sup>d</sup>Beijing Colleges and Universities Engineering Research Center of Advanced Laser Manufacturing, Beijing 100124, People's Republic of China.

E-mail: zhaoyan@bjut.edu.cn

<sup>‡</sup>These authors contributed equally to this work

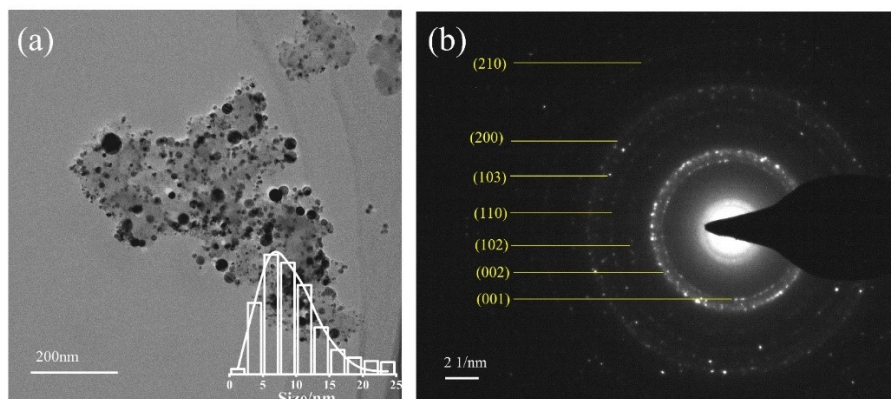


**Figure S1.** (a) TEM image of carbon-supported Pd-doped Ru NPs, (b) selected area electron diffraction (SAED) pattern of the Pd-doped Ru NPs.

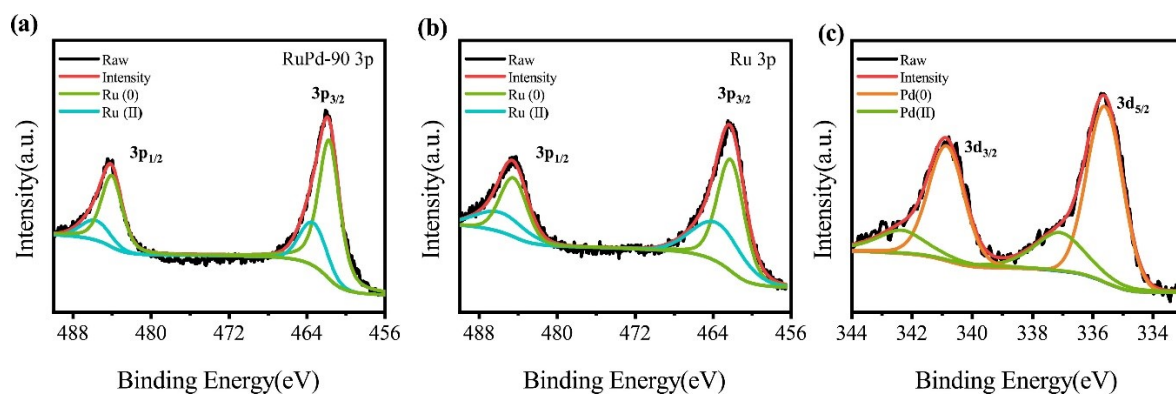


**Figure S2.** The valence distributions of (a) Ru 3p orbital and (c) Pd 3d orbital in RuPd-90, (b) Ru 3p orbital in isolated Ru NPs shown by XPS.

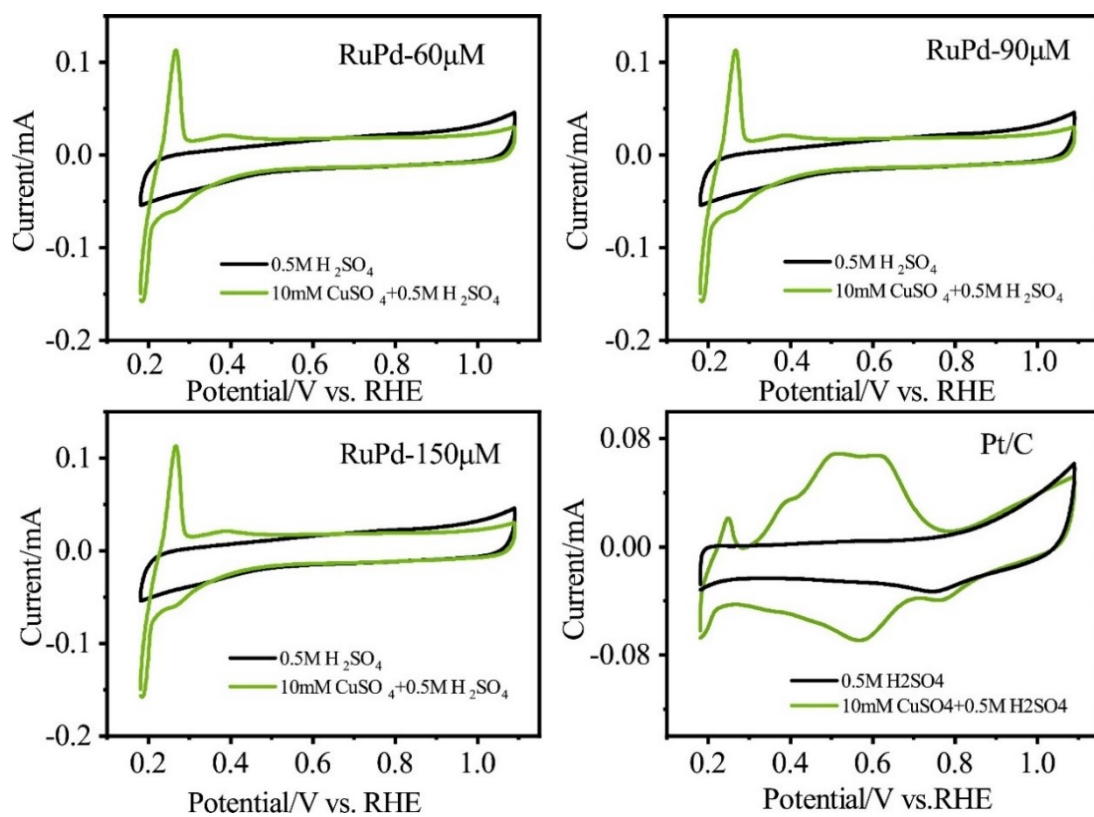


**Figure S3.** CV in different solutions on (a) RuPd-60; (b) RuPd-90; (c) RuPd-150; (d)Pt/C. Scan rate: 10 mV/s

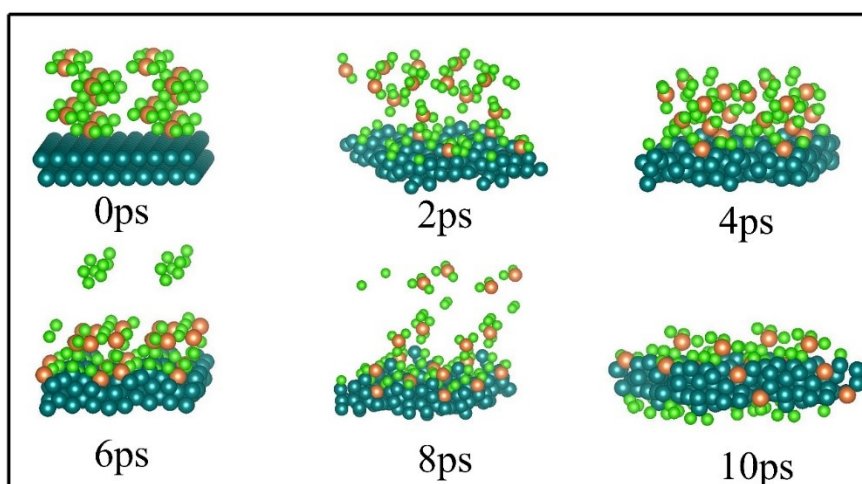


**Figure S4.** Snapshots of Pd doping carried out via MD simulation.

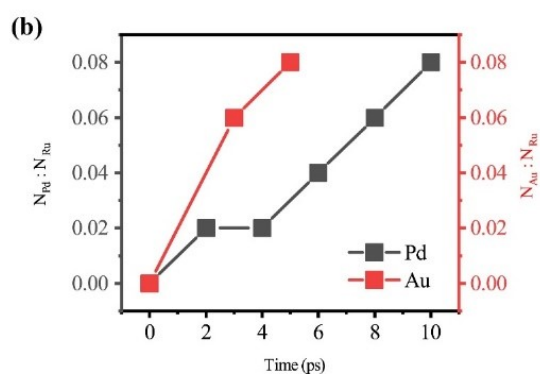
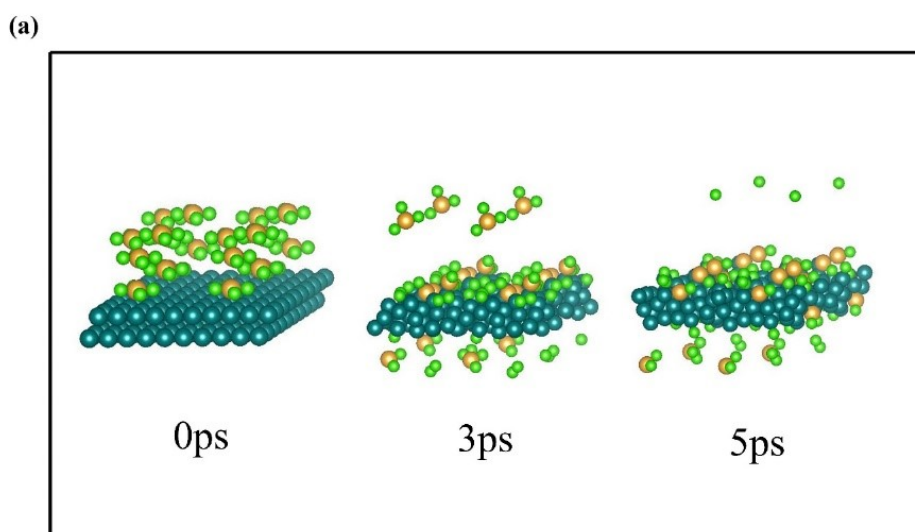


**Figure S5.** (a) Snapshots of Au doping carried out via MD simulation. (b) Doping ratio of Pd and Au embedded in Ru matrix at different times.

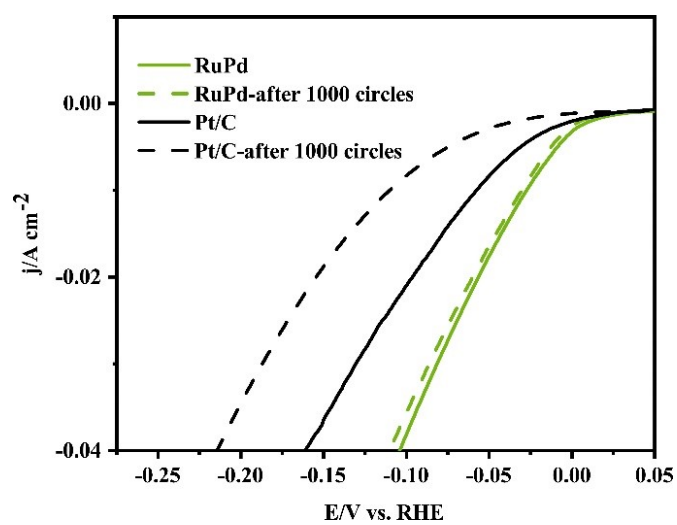


**Figure S6.** Durability test during the 1000 CV circles.

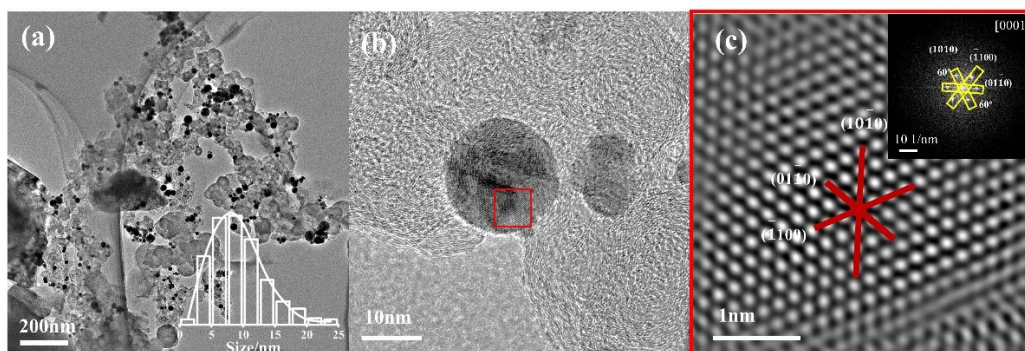


**Figure S7.** (a) TEM and (b) HRTEM images and its (c) FFT and inverse FFT images of RuPd-90 after the durability test.

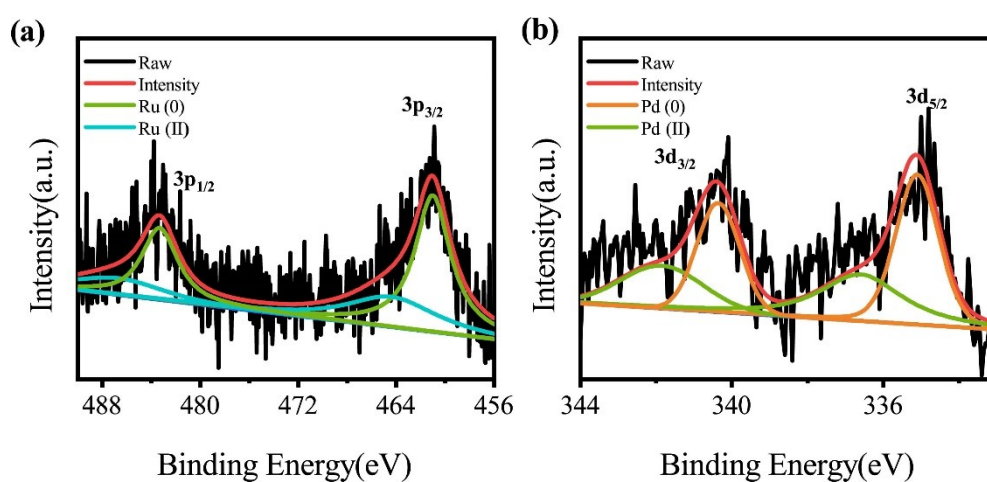


**Figure S8.** The valence distributions of (a) Ru and (b) Pd in RuPd-90 shown by XPS after the durability test.

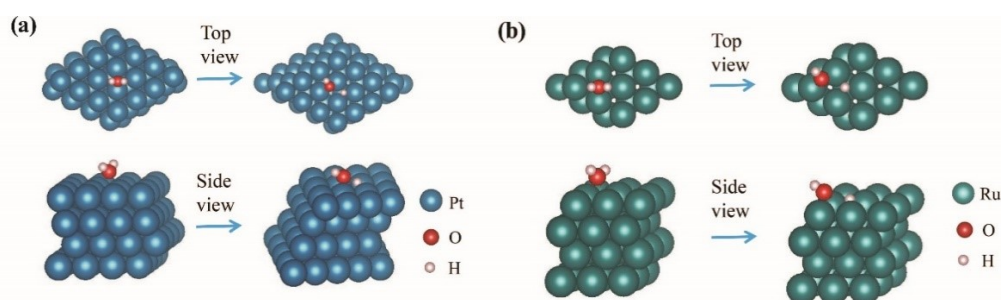


**Figure S9.** The splitting process of water molecules on atomic model of (a) Pt (111) and (b) Ru (001) facets.

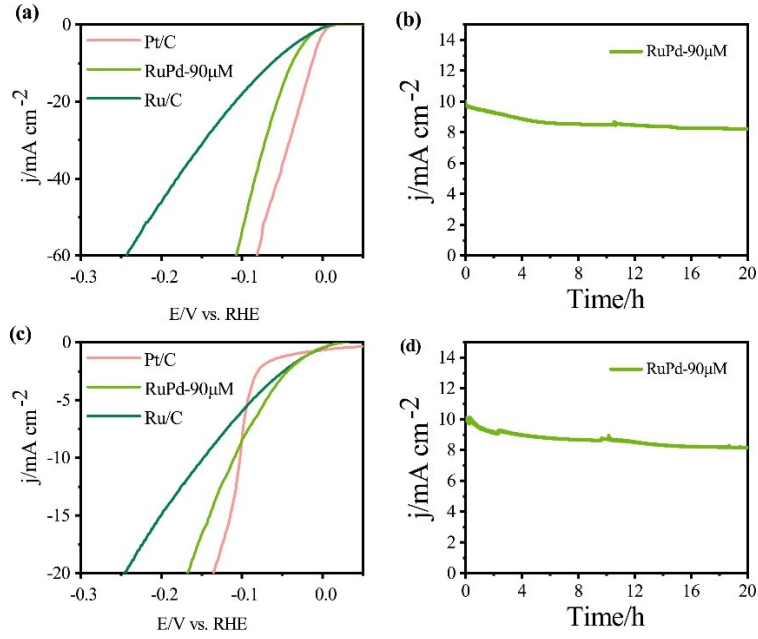


**Figure S10.** (a) LSV polarization curves with a scan rate of 5 mV/s and (b) CA curves recorded at an overpotential corresponding to the current density of 10 mA cm<sup>-2</sup> test in 0.5M H<sub>2</sub>SO<sub>4</sub>; (c) LSV and (d) CA curves test in 0.01M PBS.

**Table S1.** The list of measured overpotential values for different precursor concentrations.

C <sub>H<sub>2</sub>PdCl<sub>4</sub></sub> (μM)	Test					average
	1	2	3	4	5	
60	31mV	30mV	29mV	29mV	30mV	30mV
90	27mV	24mV	28mV	27mV	29mV	27mV
150	37mV	37mV	39mV	37mV	38mV	37mV
200	49mV	49mV	49mV	50mV	49mV	49mV
300	52mV	50mV	49mV	50mV	50mV	50mV

**Table S2.** The list of measured m<sub>Ru</sub>:m<sub>Pd</sub> values for different precursor concentrations.

C <sub>H<sub>2</sub>PdCl<sub>4</sub></sub> (μM)	Test			average
	1	2	3	
60	21:1	18:1	19:1	19:1
90	15:1	17:1	15:1	15:1
150	13:1	12:1	12:1	12:1
200	9:1	9:1	8:1	9:1
300	8:1	9:1	8:1	8:1